

Plasma Ion Diagnostics Using Resonant Fluorescence

R. A. Stern

Bell Laboratories, Murray Hill, New Jersey 07974

and

J. A. Johnson, III

Department of Physics, Rutgers University, New Brunswick, New Jersey 08903

(Received 21 April 1975)

Laser-induced fluorescence of ionic states is used to measure local ion densities and velocities in argon plasmas.

We present experimental tests of a sensitive diagnostic method with wide applicability in plasma and fluid physics, together with new results obtained through its use. The technique addresses itself to an essential current problem¹: the remote, noninterfering measurement of collective ion properties (density and velocity distribution). Tests summarized below show that laser fluorescence spectroscopy is superior to methods now in use with respect to spatial resolution and ability to probe the ion distribution.

Various ways of using resonant laser excitation of ions in plasmas have been conceptually explored.² The basic parameter underlying such processes is the probability for excitation per particle, $P = \int N(\nu)\sigma(\nu)d\nu$. Here the absorption cross section $\sigma(\nu)$ at resonance³ tends to the limit $\lambda^2/8\pi \sim 10^{-11} \text{ cm}^2$ for wavelengths λ in the visible, and is many orders of magnitude larger than the Thomson or Raman cross sections. A photon flux density $N(\nu) = 10^{11} \text{ cm}^{-2} \text{ sec}^{-1} \text{ Hz}^{-1}$ then suffices to ensure excitation probabilities of order unity (saturation), e.g., using a cw argon-II laser with 0.5 W focused to 0.5 mm.

Experiments were carried out in low-pressure hot-cathode dc discharges in argon, which belong to an important physical configuration: plasmas supporting strong electrostatic fields. In such systems, when collision probabilities are low, an ion initially at rest will acquire the mean speed $v = e|\vec{E}|\tau/M$ along the axis of the field \vec{E} during the mean-free time τ between collisions. Small-impact-parameter (large-angle) collisions with heavy particles (neutral or ionized) randomly redistribute a large fraction—typically $\frac{1}{2}$ —of this speed in the plane normal to \vec{E} . The ions thus end up acquiring field-dependent transverse pseudotemperatures, i.e., random distributions of speeds $v_{\perp} \approx nv$, where n ranges from 0.5 to 3 typically, which greatly exceed equilibrium val-

ues. Theory predicts that in the resulting anisotropic distribution function $f(\vec{v})$, ions with large axial (drift) velocities also end up with large transverse speeds (pseudotemperatures) v_{\perp} .

In the tests, singly ionized argon was excited by the intense radiation at 4880 Å (transition $4p^2 D_{5/2} \rightarrow 4s^2 P_{3/2}$) from a single-line Ar-II laser. The discharge operated at pressures down to 4 mTorr, currents up to 5 A, and average dc field strengths 3 to 4 V/cm, in an 8-mm-i.d. Pyrex or quartz tube with a Helmholtz axial magnetic field of typically 50 G. The ground-state ion density could be varied up to $5 \times 10^{11} \text{ cm}^{-3}$, with a "target" $4s^2 P_{3/2}$ excited-state density estimated at 10^6 cm^{-3} or less. Stark and collisional line-perturbing effects were negligible and the medium remained optically thin at all lines used. Along the laser beam, ions in the initial state $4s^2 P_{3/2}$ were excited into the upper state $4p^2 D_{5/2}$. Ions in this upper state can decay either to the $4s^2$ state with emission of a 4880-Å photon ($\tau \approx 10$ nsec), or to the $4s^4 P_{3/2}$ state with emission of a photon at 4228 Å ($\tau \approx 100$ nsec). Thus the fluorescent emission of either 4880- or 4228-Å radiation, following excitation by the laser beam, provides a diagnostic of the condition of a target ion.

To optimize spatial resolution—an essential advantage of the active technique used here over the usual, passive optical methods¹—the laser beam was focused to a 0.5 mm diam and the diagnostic region viewed through an $f/3.5$ lens system along an axis normal to the laser beam focused on the beam waist. A variable slit in the image plane limited the extent of the diagnostic volume, whose dimensions were therefore determined by the product of laser-beam area and slit width. Typically with a 3-mm slit the observed fluorescence originated within a volume of 10^{-3} cm^3 .

To discriminate between fluorescence and

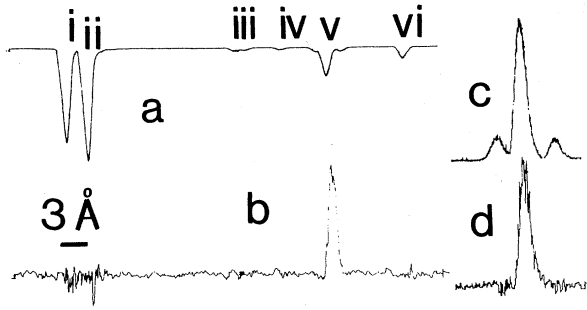


FIG. 1. Spontaneous (traces *a* and *c*) and fluorescent (traces *b* and *d*) spectra of argon-gas discharge, pressure 8 mTorr, discharge current 4 A. Vertical axes: intensity, linear scale, relative units. Horizontal axes: wavelength, linear scale. Prominent lines are (i) 4198.3, (ii) 4200.7 Å from Ar I; (iii) 4218.7, (iv) 4222.6, (v) 4228.16, and (vi) 4237.22 Å from Ar II. 0.25-m grating monochromator (1800 lines/mm) with 100- μ m slit for traces *a* and *b*, 30- μ m slit for traces *c* and *d*. In *a*, more light corresponds to downward trace deflection.

spontaneous emission, the laser was intensity modulated. Figure 1, trace *a*, presents the spontaneous emission from the plasma over the spectral range 4190 to 4240 Å, containing several lines. In contrast, in Fig. 1, trace *b*, the abscissa is proportional to the amplitude of the photodetector component phase locked to the laser modulation frequency. Here, only the 4228-Å ion line is seen to have a measurable amplitude. On an expanded scale the ion lines at 4227 and 4229.9 Å (-1.1 and +1.7 Å from the 4228-Å center) are clearly visible in emission *c*, but do not appear in the fluorescence spectrum *d*. This resolving power of the technique indicates that simple, "open" optics can be used, since competition from unwanted lines can be negligible.

The connection between the target and ground (majority) ionic state is illustrated in Fig. 2. The lower trace (circles) is a plot of the fluorescence intensity averaged over the 4228-Å line as a function of the discharge current I_{dc} . The quadratic dependence indicates that the $4s^2$ state originates in collisions between energetic electrons and ground-state ions. This result is consistent with indirect measurements and calculations. The upper trace (squares) is a plot of the current dependence of the 4228-Å spontaneous emission. This monitors the $4p$ -state population, known to originate from electron-ground-state-ion collisions, and expected to be proportional to I_{dc}^2 as shown here.⁴ We conclude that the laser-induced fluorescence is a sensitive probe of the

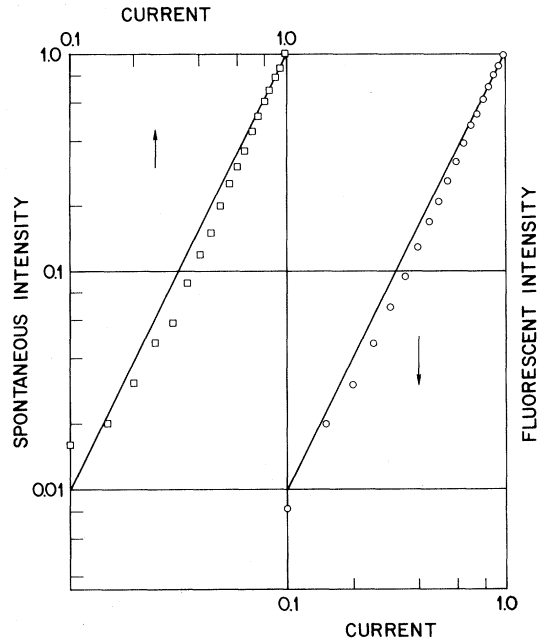


FIG. 2. Spontaneous (squares) and fluorescent (circles) intensity of Ar II line at 4228 Å versus discharge current. Laser beam is parallel; radiation is viewed normal to discharge axis. Vertical axes: intensity, log scale. Horizontal axes: discharge current, normalized to 2.0 A.

local majority-ion density.

The narrow linewidth $\Delta\lambda$ and strong collimation (small wave-number spread) in laser beams enable the ion velocity distribution to be sampled in plasmas, such as low-pressure discharges, where the linewidth of ionic spectral lines is attributable to the Doppler spread due to $f(\vec{v})$. A resonant laser beam will selectively excite only the fraction of ions whose velocity component v along the laser beam is less than $v_{max} = \Delta\lambda c/\lambda$. Thus, depending on the angles between laser beam, viewing axis, and field gradients, different sections of the velocity distribution can be probed.

Under our conditions, the laser linewidth of 0.02 Å corresponds to $v_{max} = 1.2 \times 10^5$ cm sec⁻¹. Using the collision cross section⁵ $\sigma_{A,A^+} = 1.34 \times 10^{-14}$ cm², a typical mean speed $v \cong 1.7 \times 10^5$ cm sec⁻¹ is calculated. We expect therefore to find largely different $v_{\perp} \approx nv$ (typically $0.5 < n < 3$) depending on the angle between laser and field axis.

Figure 3 demonstrates the selectivity of the laser-fluorescence diagnostic through two examples. First, Fig. 3, trace *a*, shows the fluorescent-line detail at 4880 Å, with the laser beam

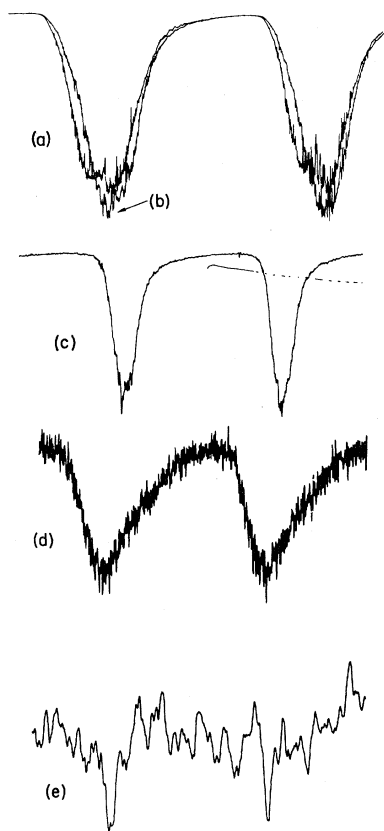


FIG. 3. Detailed (Fabry-Perot) spectra of Ar II line at 4880 Å. More light corresponds to downward trace deflection. (a) Fluorescence with laser beam normal to discharge axis; (b), (c), laser line, free spectral range (distance between peaks) 0.2 Å; (d) spontaneous emission (viewed normal to discharge axis); (e) fluorescence with laser beam parallel to discharge axis.

incident on the plasma at *right angles* to the field axis. The viewing axis is normal to the field, so that the detector is sensitive to the transverse velocity spread v_{\perp} of the fluorescent ions. The superposed trace *b* shows the laser line alone. The fluorescent line (trace *a*) is only slightly wider, indicating that the laser has excited all those ions whose transverse velocities are less than v_{\max} and hence lie within the laser linewidth.

Trace *c* is a laser-line profile providing calibration for traces *d* and *e* below; the free spectral range of 0.2 Å determines the distance between line centers. The large width of the spontaneous line *d*, about 0.09 Å, corresponds to transverse velocities as large as 5×10^5 cm sec⁻¹ $\cong 3v$ (as predicted theoretically) and equivalent to a 6 eV "temperature."

Finally, trace *e* presents the fluorescence, viewed normally to the field, but with the laser

beam *parallel* to the field axis. Here $E/p \sim 600$ V/cm Torr corresponds⁵ to an average drift speed 2×10^5 cm sec⁻¹, appreciably larger than v_{\max} , so that the average ion distribution is detuned from the laser line. The low signal-to-noise ratio indicates that only a small fraction of the $4s^2$ ions now fluoresce. Most significantly, the linewidth is much narrower than either the spontaneous or laser lines. This unique condition indicates, as expected, that ions with low v_{drift} have transverse speeds v_{\perp} which are much less than the mean spread (trace *d*), and can even be lower than the maximum Doppler speed allowed by the laser gain envelope ($v_{\perp} \approx 0.5 V < v_{\max}$).

These results, which verify qualitatively some physical aspects predicted by well-known theoretical treatments, illustrate the versatility of the laser-fluorescence technique. They suggest that, using the particular properties of lasers, one can diagnose density and velocity spectra not attainable by other means.

The technique just described is applicable to a wide variety of plasmas of high current interest. Of course it is immediately useful in argon plasmas, which comprise a very large fraction of plasmas used in current basic research.⁶ It is trivially extendable to other gases as well as to alkali plasmas,⁷ using commercial tunable lasers.² It is also directly applicable to thermonuclear studies, e.g., in relativistic-electron-beam plasmas and tokamak-like geometries with impurities, where the plasmas contain excited-state ion populations (typically in He, Ar, or N) which fluoresce in the visible.⁸

It is a pleasure to acknowledge useful discussions with H. M. Gibbs, K. B. McAfee, C. K. N. Patel, and G. D. Patterson.

¹Currently used optical techniques are illustrated in W. L. Wiese, D. E. Kelleher, and N. R. Paquette, *Phys. Rev. A* **6**, 1132 (1972); D. E. Kelleher and W. L. Wiese, *Phys. Rev. Lett.* **31**, 1431 (1973); D. E. Evans and M. L. Yeoman, *Phys. Rev. Lett.* **33**, 76 (1974); J. P. Van Devender, J. D. Kilkenny, and A. E. Dangor, *Phys. Rev. Lett.* **33**, 689 (1974); N. Rynn, D. R. Dakin, D. L. Correll, and G. Benford, *Phys. Rev. Lett.* **33**, 765 (1974); D. J. Sigmar, J. F. Clarke, R. V. Neidigh, and K. L. Vander Sluis, *Phys. Rev. Lett.* **33**, 1376 (1974).

²R. M. Measures, *J. Appl. Phys.* **39**, 5232 (1968), and *J. Quant. Spectros. Radiat. Transfer* **10**, 107 (1970); C. B. Wheeler and J. Troughton, *Plasma Phys.* **11**, 391 (1969); D. Dimock, E. Hinnov, and L. C. Johnson,

Phys. Fluids **12**, 1730 (1969).

³Excluding statistical weight and lifetime factors, which can be of order units. H. J. Andrä, A. Gaupp, and W. Wittmann, Phys. Rev. Lett. **31**, 501 (1973); A. C. G. Mitchell and M. W. Zemansky, *Resonance Radiation and Excited Atoms* (Macmillan, New York, 1934).

⁴V. F. Kitaeva, A. N. Odintsov, and N. N. Sobolev, Usp. Fiz. Nauk **99**, 361 (1969) [Sov. Phys. Usp. **12**, 699 (1970)]; A. I. Imre, A. I. Daschenko, I. D. Zape-sochny, and V. A. Kel'man, Pis'ma Zh. Eksp. Teor. Fiz. **15**, 712 (1972) [JETP Lett. **15**, 503 (1972)].

⁵G. H. Wannier, Phys. Rev. **83**, 281 (1951), and **87**, 795 (1952); J. A. Hornbeck, Phys. Rev. **84**, 615 (1951).

⁶Typical current uses of argon plasmas in basic studies are illustrated by S. Bernabei, M. A. Heald, W. M. Hooke, and F. J. Paoloni, Phys. Rev. Lett. **34**, 866 (1975); A. Y. Wong and R. L. Stenzel, Phys. Rev. Lett. **34**, 727 (1975); D. Gresillon and F. Doveil,

Phys. Rev. Lett. **34**, 77 (1975); C. A. Primmerman, L. M. Lidsky, and H. D. Politzer, Phys. Rev. Lett. **33**, 957 (1974); H. C. Kim, R. L. Stenzel, and A. Y. Wong, Phys. Rev. Lett. **33**, 886 (1974); N. Hershkowitz, T. Romesser, G. Knorr, and C. K. Goertz, Phys. Rev. Lett. **33**, 754 (1974); etc.

⁷Illustrative current uses of alkali plasmas can be found in N. Sato, H. Sugai, and R. Hatakeyama, Phys. Rev. Lett. **34**, 931 (1975); M. Yamada, H. W. Hendel, S. Seiler, and S. Ichimaru, Phys. Rev. Lett. **34**, 650 (1975); H. Sugai and E. Märk, Phys. Rev. Lett. **34**, 127 (1975); J. A. Schmidt, N. R. Sauthoff, and R. J. Hawryluk, Phys. Rev. Lett. **33**, 1217 (1974); etc.

⁸See, for instance, C. A. Kapetanacos, W. M. Black, and K. R. Chu, Phys. Rev. Lett. **34**, 1156 (1975); G. C. Goldenbaum, W. F. Dove, K. A. Gerber, and B. G. Logan, Phys. Rev. Lett. **32**, 830 (1974); S. Hidekuma, S. Hiroe, T. Watari, T. Shoji, T. Sato, and K. Takayama, Phys. Rev. Lett. **33**, 1537 (1974); Ref. 1 above.

Anti-Stokes Light Scattering by a Band-to-Band Transition in GaSb[†]

G. Benz and R. Conradt

Physikalisches Institut der Universität Stuttgart, D-7000 Stuttgart-80, Federal Republic of Germany

(Received 18 February 1975; revised manuscript received 29 April 1975)

A new emission band at about $h\nu = 2$ eV is observed in GaSb which is excited by a Nd-yttrium aluminum garnet laser. From the dependence on the crystal orientation and integrated intensity and from the line shape and its dependence on doping, it is concluded that the emission band cannot be attributed to nonlinear mixing of the laser line with the E_g luminescence, but is caused by electronic interband anti-Stokes Raman scattering.

In GaSb, excited by a Q-switched Nd-yttrium aluminum garnet (YAIG) laser, two emission bands appear lying energetically between the laser energy and the second harmonic of the laser line. One emission band is located at about $h\nu = 1.58$ eV, the other one at about $h\nu = 2$ eV. The first band is attributed to the radiative recombination of Auger-excited holes in the split-off valence band with free or shallow-bound conduction-band electrons and was reported earlier.¹ In this paper we report the new band at about $h\nu = 2$ eV which is about two orders of magnitude weaker than the Auger band.

GaSb crystals are immersed in liquid He and are excited by a Q-switched Nd-YAIG laser, focused on the sample to a peak power density of about 100 kW cm^{-2} . A minority-carrier density of about 10^{17} cm^{-3} at the crystal surface is estimated. The samples used in the experiments are undoped p-type and Te-doped n-type single crystals. The luminescence is dispersed by a 0.85-

m Spex double spectrometer and is detected with an RCA C31034A photomultiplier with GaAs cathode using a "digital-boxcar-integration" method described elsewhere.² All spectra are corrected for the spectral response of the system and for the transfer from the wavelength scale to the energy scale. Furthermore, the spectra measured above the bandgap are corrected for reabsorption in the sample. Figure 1 shows the spectra of a not intentionally doped GaSb sample [$p(300 \text{ K}) = 1.2 \times 10^{17} \text{ cm}^{-3}$] at 4.2 K in the energy range 1.4 to 2.4 eV. The upper part is the result on a (111)-oriented surface. The lower part is obtained from a (100)-oriented surface. The band at 1.58 eV is the known Auger band.¹ The second harmonic of the laser lies at 2.33 eV. Between these lines the new comparably weak band appears at about 2 eV.

As an explanation of the new band, any type of two-step excitation to another band extremum—as is the case for the 1.58-eV band, for exam-